Study on Low Temperature Oxidation with a Separated Cool flame of *n*-Heptane in a Micro Flow Reactor with a Controlled Temerature profile

R. Tatsumi[1], H. Nakamura[1], S. Hasegawa[1], T. Tezuka[1], K. Maruta[1,2]
[1]Institute of Fluid Science, Tohoku University, Sendai city, Miyagi prefecture, Japan
[2]ICE Lab. , Far Eastern Federal Univercity, Russky Island, Vladivostok, Russia

1 Introduction

n-Heptane is one of the primary reference fuels of gasoline which exhibit low-temperature oxidations. Thus, ignition characteristics of *n*-heptane have been extensively investigated [1-3]. However, it has been pointed out that prediction capability for low-temperature oxidation of existing chemical kinetics is not sufficient because of the lack of experimental data and long reaction time scale of low-temperature ignition phenomena. That is, mere examination on the ignition delay time is insufficient for developing highly precise chemical kinetics for low-temperature oxidation. Here, a micro flow reactor with a controlled temperature profile (MFR) [4, 5, 6] is applied as novel methodology for examining low-temperature oxidation of *n*-heptane. In MFR, weak flame can be obtained at very low flow velocity condition, and it has been utilized for examining ignition characteristics of given mixture [5]. Therefore, special attention is paid to weak flames of *n*-heptane/air mixture in MFR in this study. MFR system is composed of a quartz tube, whose diameter is smaller than the ordinary quenching diameter, and an external heat source. The external heat source creates the stationary temperature profile on the inner surface of reactor tube in the flow direction. Our previous study reported that multiple weak flames were observed in MFR when *n*-heptane/air mixtures was applied [6]. This interprets that general transient multi-stage ignition phenomena can be observed as spatially separated steady three weak flames in MFR. These three weak flames correspond to cool, blue and hot flames. In this study, the first attempt to separate a steady cool flame from multiple weak flames will be made and chemical structure of single cool flame in MFR will be investigated by species measurements.

2 Experimental and computational method

Weak flame observation and species measurements in MFR were conducted. A schematic of the experimental setup for weak flame observation is shown in Fig. 1.a. A quartz tube whose inner diameter is 2 mm was used as a reactor and *n*-heptane/air mixture at ϕ=1 was supplied to the reactor. The vertical type reactor was adopted to attain symmetric weak flame in lower temperature gradient profile. Maximum wall temperatures ($T_{w,max}$) were controlled in the range of 700 to 1300 K by manipulating hydrogen burner setting. By varying $T_{w,max}$, it is supposed that oxidation process in the stationary temperature gradient can be

Correspondence to: tatsumi@edyn.ifs.tohoku.ac.jp

controlled. After examining the optimum $T_{w,max}$, species measurements at the exit of MFR will be made to investigate chemical structure of separated cool flame. A schematic of the experimental setup for the species measurements is shown in Fig. 1.b. Time-of-flight mass spectrometer (TOF/MS) with electric ionization was employed as a gas analyzer. To precisely control $T_{w,max}$ in relatively low temperature conditions, electric heater with ambient flow was employed as an external heat sources in the species measurements. One-dimensional steady-state code based on PREMIX was used for computation. A convective heat transfer term between gas phase and wall was added to the energy equation [4]. Three mechanisms (KUCRS [7], LLNL [8], MFL [9]) were used to examine their performances in MFR. Flame positions are defined as heat release rate (HRR) peak positions and computations were conducted in the same conditions as those of experiments.

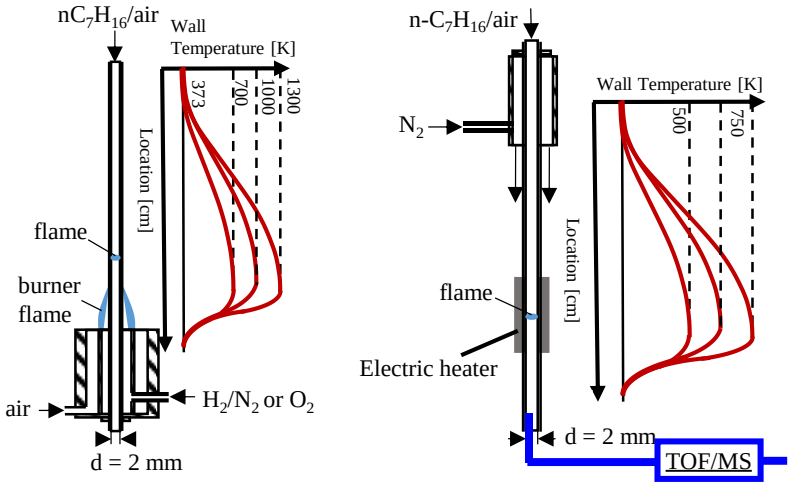

Fig. 1 schematic of experimental setup for flame observation (left : 1.a), and species measurements (right : 1.b)

3 Results and discussion

3.1 Flame observation

The experimental weak flame image and computational weak flame structure of stoichiometric *n*-heptane/air mixture in MFR calculated by KUCRS mech. at $T_{w,max}$ = 1300 K is shown in Fig. 2.a. Locations of three experimental luminous zones are in good agreements with those of computational multiple weak flames defined as three peaks of HRR. In the first weak flame, *n*-heptane is consumed and CH_2O and H_2O_2 are produced. These species formations are typical to cool flame. In the second weak flame, CH_2O and H_2O_2 are consumed and significant amount of CO is produced. In the third weak flame, CO is consumed and CO_2 is produced. From these phenomena, we could confirm the three experimental weak flames in flow direction are cool, blue and hot flames which are the same as our previous results [6]. From Fig. 2a, cool flame is found to locate at wall temperature from 600 K to 700 K. Based on this information, further experiments and computations are conducted by selecting $T_{w,max}$ = 700 K to stabilize a separated cool flame in MFR. The experimental weak flame image and computational weak flame structure calculated by KUCRS mech. at $T_{w,max}$ = 700 K is shown in Fig. 2.b. It is clearly shown in the figure that single luminous zone is obtained this time. The position of experimental weak flame is in good agreement with that of computational HRR peak. At this flame, *n*-heptane is consumed and CH_2O and H_2O_2 are produced similar to the first weak flame when $T_{w,max}$ = 1300 K. It is confirmed that blue flame reactions which consume cool flame products and produce CO are not observed. Therefore observation of steady separated cool flame is successfully achieved in MFR if $T_{w,max}$ = 700 K is selected.

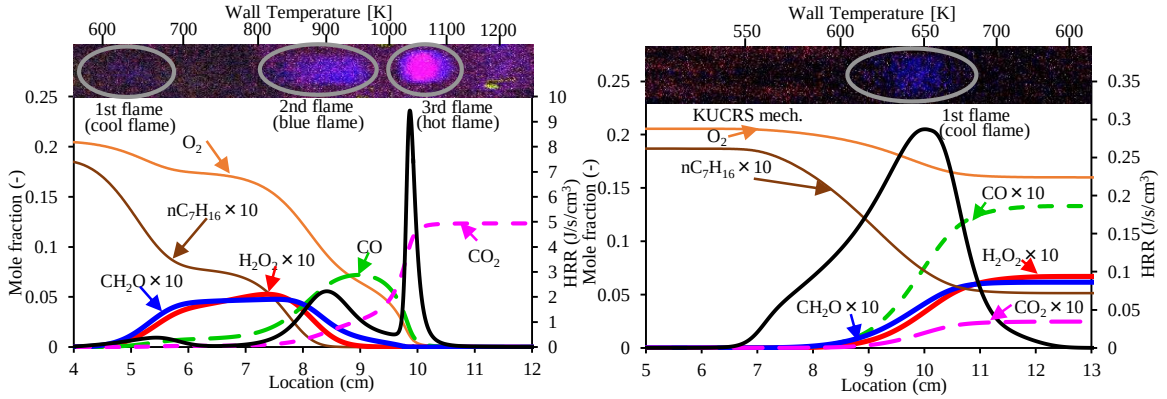

Fig. 2 experimental weak flame images and computational weak flame structures calculated by KUCRS mech. at $T_{w,max}$ = 1300 K (left : 2.a) and at $T_{w,max}$ = 700 K (right :2.b).

3.2 Characteristics of steady separated cool flame

OH radicals play important roles in cool flame. Thus special attention was paid to OH radicals here. Profiles of the top three reactions in OH production and consumption are shown in Fig. 3.a. OH is mainly produced by radical branching path which produce ketohydroperoxide (decomposed into aldehydes and ketone group) and by radical propagation path which produces cyclic ethers (decomposed into alkenes and ketone group). These two paths which consume hydroperoxy-alkyl radical are competing. On the other hand, OH is mainly consumed by the fuel decomposition reactions, particularly where cool flame formation is started. That is to say, there is radical chain cycle between the two paths and fuel decomposition reaction so that the two paths are significantly contributed to the cool flame formation. Comparison between profiles of net rates of OH production by radical branching and radical propagation paths and the OH mole fraction profile are shown in Fig. 3.b to examine which path is dominant in cool flame formation. Radical branching path produces large amount of OH, but radical propagation path doesn't contribute to net rates of OH production.

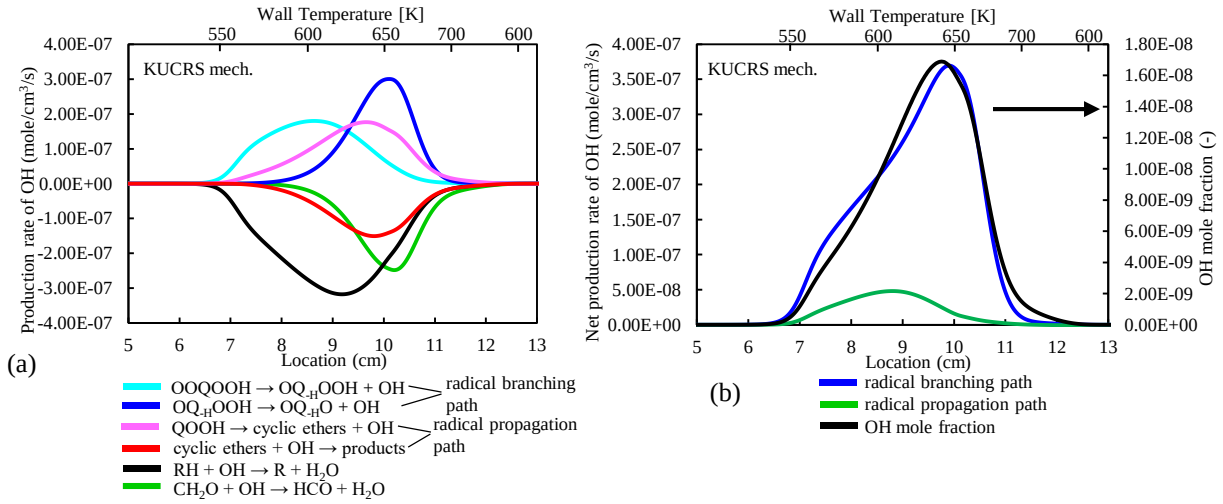

Fig. 3 Profiles of top three reactions in OH production and comsumption (left : 3.a) and profiles of net rates of OH production by radical branching and propagation paths and OH mole fraction profiles from different reaction mechanisms (right : 3.b).

Furthermore the shape of net rates of OH production in radical branching path and that of OH mole fraction profile are qualitatively in good agreement with each other. Therefore, significant correlation between radical branching path and cool flame formation is seen. In other words, it is very important for cool flame chemistry to evaluate the ratio of radical branching path to radical propagation path in such a low temperature conditions.

3.3 Species measurements

In the present study, measurements of *n*-heptane, CO, CO_2, CH_2O, C_2H_4, C_3H_6, CH_3CHO and $C_7H_{14}O$ (cyclic ethers) were conducted. Radical branching path mainly produces aldehydes and ketone group, and radical propagation path mainly produces alkenes and ketone group, as discussed in the above section. CH_3CHO is regarded as representative species of the radical branching reactions and C_2H_4, C_3H_6 and $C_7H_{14}O$ are regarded as representative species of the radical propagation reactions. Profiles of normalized major species mole fractions are shown in Fig. 4. Special attention was paid to overall shape of the species profiles and the temperature levels where species reaction starts. This is because the former and latter are indicators of the progress and start of low-temperature oxidation reactions. *n*-Heptane experimental results show *n*-heptane mole fraction starts to decrease around $T_{w,max}$ = 570 K and rapidly decreases above $T_{w,max}$ = 580 K and then it is slightly increased if $T_{w,max}$ is higher than 670 K. Experimental results of CO, CO_2, and CH_2O show production of CH_2O starts at lowest temperature at $T_{w,max}$ = 565 K among them, and productions of CO and CO_2 follow. Once productions of CO and CH_2O occur, profiles of these species show similar tendencies that have sharp increases and then constant mole fractions at $T_{w,max}$ > 670 K. Overall shapes of the major species profile in experiments show fair qualitative agreements with computational results except for the temperature levels where initial consumption and production start. This temperature level with KUCRS mech. for CO CO_2, and CH_2O show better agreements with those of experiments than two other reaction mechanisms. However, KUCRS mech. did not reproduce experimental tendencies at higher $T_{w,max}$. Profiles of normalized mole fractions of representative species for radical branching path (CH_3CHO) and radical propagation path (C_2H_4, C_3H_6 and $C_7H_{14}O$) are shown in Fig. 5. Results of measured CH_3CHO show similar tendencies with those of CO CO_2, and CH_2O in Fig. 4. However, representative species for radical propagation path show different tendencies with CH_3CHO. Measured C_2H_4 and C_3H_6 mole fractions show monotonic increase and their gradients change at around $T_{w,max}$ = 650 K. Measured $C_7H_{14}O$ show specific tendency. At first, production of $C_7H_{14}O$ is seen at $T_{w,max}$ = 565 K and then mole fraction of $C_7H_{14}O$ attains a peak at slightly above 600 K. After showing a local minimum around $T_{w,max}$ = 660 K, it increases again when $T_{w,max}$ > 670 K and continues to increase within the temperature range addressed here. In contrast to the major species, large discrepancies are seen between experiments and computations especially in CH_3CHO and $C_7H_{14}O$ profiles. In CH_3CHO profiles, experimental result shows monotonic increase and constant region in its profile but computational results with all mechanisms show an obvious peak in their profiles. In $C_7H_{14}O$ profiles, overall trend with KUCRS mech. is significantly different from experimental results. In the case of MFL mech., maximum amount of $C_7H_{14}O$ is attained around $T_{w,max}$ = 605 K but that of experimental result is seen around the highest wall temperature addressed here, i.e., $T_{w,max}$ = 750 K. Overall shapes of C_2H_4 and C_3H_6 with LLNL and MFL mech. are in better agreements with those of experiments among three mechanisms but temperature level where production starts of C_2H_4 and C_3H_6 with KUCRS and MFL mech. are in fair agreement with those of experiments. From Figs. 4 and 5, it can be concluded that experimental overall shapes of major and representative species except for $C_7H_{14}O$ when $T_{w,max}$ > 650 K show the best agreement with the results of MFL mech. and experimental temperature levels where most of the species production starts show the best agreements with the results of KUCRS mech. By using the sampling results in MFR, predictivity of low-temperature oxidation by reaction mechanisms will be improved in the future.

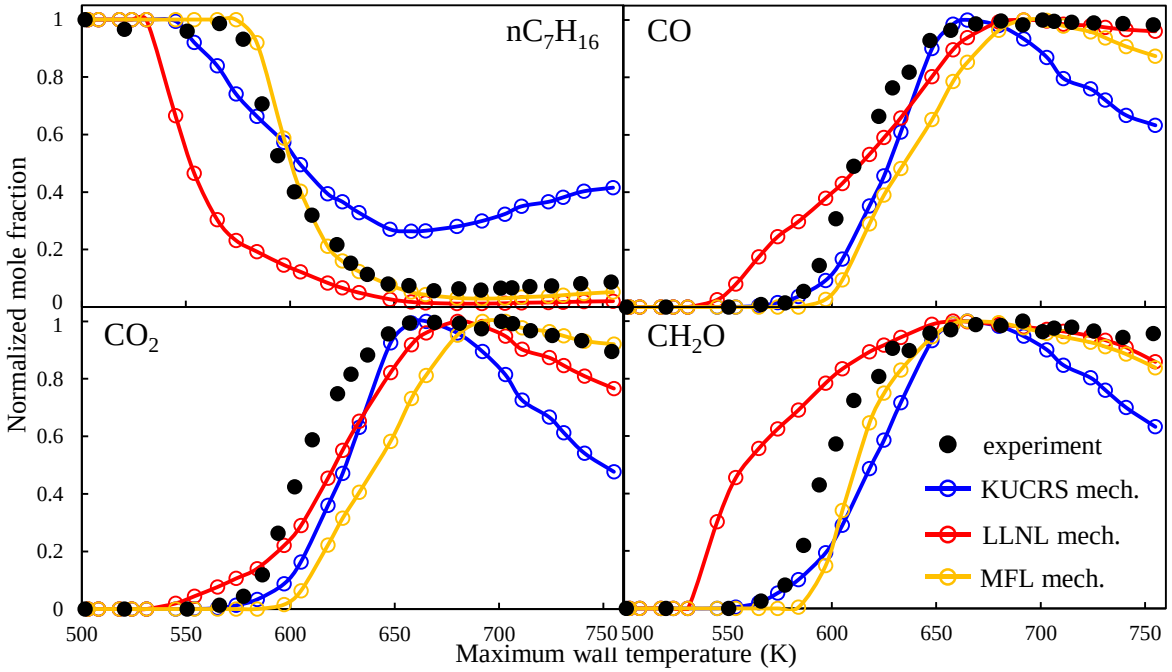

Fig. 4 Profiles of normalized mole fractions of major species.

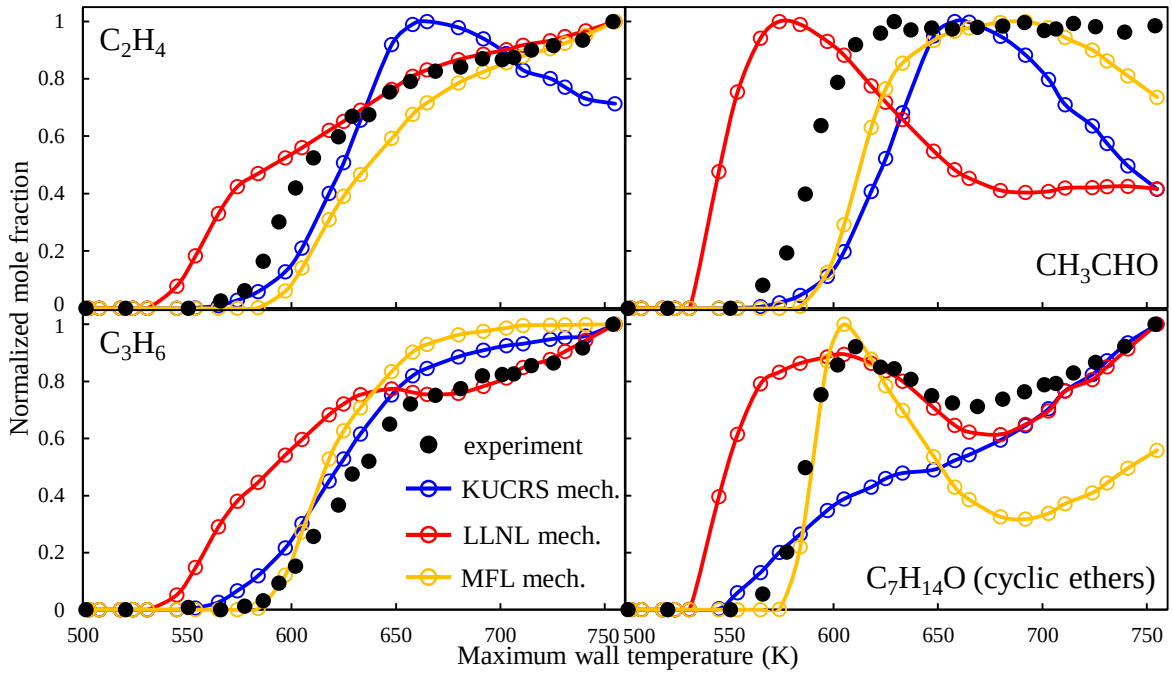

Fig. 5 Profiles of normalized mole fractions of representative species for radical branching path (CH_3CHO) and radical propagation path (C_2H_4, C_3H_6 and $C_7H_{14}O$).

4 Conclusions

A steady separated cool weak flame of stoichiometric *n*-heptane/air mixture and its chemical structure were investigated using micro flow reactor with a controlled temperature profile with species measurements and computations. Stabilization of single cool flame in the MFR was achieved by varying maximum wall temperature formed in MFR. By paying special attention to OH production and consumption reactions of low-temperature oxidation in the case of $T_{w,max}$ = 700 K, it was found that cool flame formation is strongly related to the radical branching path because there exists chain cycle between fuel decomposition reactions which consume large amount of OH and radical branching reactions which produce large amount of OH. Species measurements showed that profiles of normalized mole fractions of major species were qualitatively reproduced by the employed three reaction mechanisms except for the temperature levels of the starts of initial reactions. On the other hand, profiles for representative species of radical branching and propagation paths could not be well predicted by the present computations. It is implied that performances of chemical kinetics for low-temperature oxidation would be improved by using the species measurements in the present MFR method.

5 Acknowledgements

This work was partially supported by Council for Science, Technology and Innovation (CSTI), Cross-ministerial Strategic Innovation Promotion Program (SIP), Innovative Combustion Technology (Funding agency: JST). And the part of the study was supported financially by the Ministry of education and science of Russian Federation (project 14.Y26.31.0003).

References

[1] H.J. Curran, P. Gaffuri, W.J. Pitz, C.K. Westbrook. (1998). A Comprehensive Modeling Study of *n*-Heptane Oxidation. Combust. Flame 114 (1-2): 149.

[2] P.G. Lignola, E. Reverchon. (1987). Cool flames. Prog. Energy Combust. Sci. 13: 75.

[3] H.K. Ciezki, G. Adomeit. (1993). Shock-Tube Investigation of Self-Ignition of *n*-Heptane-Air Mixtures Under Engine Relevant Conditions. Combust. Flame 93 (4): 421.

[4] K. Maruta, T. Kataoka, N.I. Kim, S. Minaev, R. Fursenko. (2005). Characteristics of combustion in a narrow channel with a temperature gradient. Proc. Combust. Inst. 30: 2429.

[5] Y. Tsuboi, T. Yokomori, K. Maruta. (2009). Lower limit of weak flame in a heated channel. Proc. Combust. Inst, 32: 3075.

[6] A. Yamamoto, H. Oshibe, H. Nakamura, T. Tezuka, S. Hasegawa, K. Maruta. (2011). Stabilized three-stage oxidation of gaseous *n*-heptane/air mixture in a micro flow reactor with a controlled temperature profile. Proc. Combust. Inst, 33: 3259.

[7] A. Miyoshi. (2011). Systematic computational study on the unimolecular reactions of alkylperoxy (RO2), hydroperoxyalkyl (QOOH), and hydroperoxyalkylperoxy (O2QOOH) radicals. J. Phys. Chem. A 115 (15): 3301.

[8] M. Mehl, W.J. Piz, C.K. Westbrook, H.J. Curran. (2011). Kinetic modeling of gasoline surrogate components and mixtures under engine conditions. Proc. Combust. Inst. 33 (1): 193.

[9] Diesel_nheptane_chem_MFL2015, Model Fuel Library, CHEMKIN-PRO v17.2. (2016).